Mass-independent and mass-dependent Cr isotopic composition of the Rumuruti (R) chondrites: Implication for their origin and their significance for planet formation

Ke Zhu[1*], Frédéric Moynier[1], Martin Schiller[2], Conel M. O'D. Alexander[3], Jean-Alix Barrat[4], Addi Bischoff[5], Martin Bizzarro[1,2]

[1]Institut de Physique du Globe de Paris, Université de Paris, CNRS UMR 7154, 1 rue Jussieu, Paris F-75005, France

[2]Centre for Star and Planet Formation, Globe Institute, University of Copenhagen, Øster Voldgade 5–7, Copenhagen DK-1350, Denmark

[3]Earth and Planetary Laboratory, Carnegie Institution for Science, 5241 Broad Branch Road, Washington, DC 20015, USA

[4]Univ. Brest, CNRS, UMR 6539 (Laboratoire des Sciences de l'Environnement Marin), LIA BeBEST, Institut Universitaire Européen de la Mer (IUEM), Place Nicolas Copernic, 29280 Plouzané, France.

[5]Institut für Planetologie, Westfälische Wilhelms-Universität Münster, Wilhelm-Klemm-Str. 10, D-48149 Münster, Germany

*Corresponding author: Ke Zhu, email: zhu@ipgp.fr

Re-Submitted to GCA on July 15, 2020

Abstract

Chromium (Cr) isotopes play an important role in cosmochemistry and planetary science, because they are powerful tools for dating (^{53}Mn-^{53}Cr short-lived chronometry), tracing (^{54}Cr nucleosynthetic anomalies) the origins of the materials, and studying the processes involved in volatile element fractionation and planetary differentiation (Cr stable isotopic fractionation). The foundation for using Cr isotopes is to precisely know the compositions of the various chondritic reservoirs. However, the Cr isotope composition of Rumuruti (R) chondrites remains unknown. Here, we report high-precision mass-independent (average 2SE uncertainty of ~0.02 and ~0.06 for ε^{53}Cr and ε^{54}Cr, respectively; ε indicates 10,000 deviation) and mass-dependent (uncertainty of average 0.03 ‰ for δ^{53}Cr; δ indicates 1,000 deviation) Cr isotope data for 12 bulk R chondrites of petrologic types 3-6 (included R chondrite breccias), and one R chondrite-like clast (MS-CH) in the Almahata Sitta polymict ureilite. All the R chondrites show homogeneous bulk ε^{54}Cr values, -0.06 ± 0.08 (2SD), similar only to those of the Earth-Moon system and enstatite chondrites. These first ε^{54}Cr data for R chondrites provide significant addition to the ε^{54}Cr-Δ^{17}O diagram, and position them as a potential endmember for planetary precursors. The R chondrites possess a higher ^{55}Mn/^{52}Cr of 0.68 ± 0.04 and higher ε^{53}Cr values 0.23 ± 0.05 (2SD) relative to most of other chondrite groups. This likely results from the lower (e.g. than ordinary and enstatite chondrites) chondrule abundance in R chondrites. The stable Cr isotope

composition of R chondrites is homogeneous with a $\delta^{53}Cr$ = -0.12 ± 0.03 ‰ (2SD). Combined with previous data of other groups of chondrites, we show that the stable Cr isotopic composition of all the chondrites is homogeneous with $\delta^{53}Cr$ of -0.12 ± 0.04 ‰ (2SD, N = 40) and is independent of the petrologic type and redox conditions. The lack of mass-dependent fractionation between all groups of chondrites suggests that the average chondrite $\delta^{53}Cr$ value is also representative for the initial composition all differentiated planets in the Solar System. Finally, the MS-CH clast in Almahata Sitta has a Cr isotopic composition ($\varepsilon^{53}Cr$ = 0.18 ± 0.04, $\varepsilon^{54}Cr$ = -0.16 ± 0.07, and $\delta^{53}Cr$ = -0.11 ± 0.05 ‰) that is consistent (within error) with it being an R chondrite-like clast.

1. Introduction

Chondrites which contain chondrules, matrix, Fe-Ni metal and refractory inclusions, are the most primitive rocks in the Solar System available to us (e.g., Krot et al., 2014). Because they did not melt and differentiate, they may record the information of evolution of early Solar System. Chondrites also have a bulk chemical composition that is thought to be representative of their parent bodies, and are often used to approximate the compositions of the building blocks of the terrestrial planets such as the Earth (e.g., Allègre et al., 1995). Amongst the chondrites, the Rumuruti (R) chondrites are only recognized as a new group and class in 1994 (Bischoff et al., 1994; Kallemeyn et al., 1996; Rubin and Kallemeyn, 1994; Schulze et al., 1994). The physical and chemical features of the R chondrites are reviewed in detail by Bischoff et al. (2011).

Unlike other chondrites, including carbonaceous (CC), ordinary (OC) and enstatite chondrites (EC), the R chondrites have some unusual or characteristic features : 1) most of the R chondrites are breccias that contain clasts with various degree of metamorphism; 2) they have high abundances of olivine (70 vol.%); 3) matrix and chondruls have similar abundances; 4) they formed under high oxygen fugacity conditions as demonstrated by the absence of Fe-Ni metal; 5) the size of chondrules are on average ~400 μm; 6) they have element (except for Zn and Se) abundances that are similar to those in ordinary chondrites (~0.95 times of CI chondrites); 7) they have high

TiO_2 contents in the Cr-spinels; 8) Ca-Al-rich inclusions (CAIs) are rare (Rout and Bischoff, 2008; Rout et al., 2009, 2010); 9) they have higher $\Delta^{17}O$ (mass-independent $^{17}O/^{16}O$ isotope ratios; 2.72 ± 0.31) compositions than all the other chondrite groups; 10) very primitive type 3 lithologies only exist as clasts in R chondrite breccias (Bischoff, 2008); 11) within the most primitive type 3 lithologies the chondrule-matrix complementary is well defined (Friend et al., 2017).

Combining $\Delta^{17}O$ with $\varepsilon^{54}Cr$ (the parts per 10,000 deviation of the mass fractionation corrected $^{54}Cr/^{52}Cr$ ratio from a terrestrial standard) is a powerful tool for establishing relationships between Solar System materials (Clayton and Mayeda, 1999; Trinquier et al., 2007; Warren, 2011). All known bulk Solar System materials belong to one of two reservoirs: carbonaceous-chondrite (CC) with $\varepsilon^{54}Cr$ value > 0.3 and non-carbonaceous-chondrite (NC) with $\varepsilon^{54}Cr$ value < 0.3 (Qin et al., 2010; Trinquier et al., 2007). However, the $\varepsilon^{54}Cr$ values for R chondrites are still poorly known. One of only two R chondrites with previously reported $\varepsilon^{54}Cr$ values [0.43 ± 0.09, Elephant Moraine [EET] 96026 (Qin et al., 2010)] has since been re-classified as a CV3 or an ungrouped C4/5 chondrite (Meteoritical Bulletin Database; https://www.lpi.usra.edu/meteor). The only other measured R chondrite, Northwest Africa [NWA] 753 (R3.9), -0.11 ± 0.25 (Larsen et al., 2011), has a large uncertainty that spans the $\varepsilon^{54}Cr$ values of both OCs and ECs. Furthermore, just one measured sample cannot safely be taken to represent the R chondrite parent body, since there could be some degree of $\varepsilon^{54}Cr$ variability within a chondrite parent body as already observed for

CV, CO, and CM chondrites (Qin et al., 2010; Trinquier et al., 2007). Apart from the one relatively imprecise ε^{54}Cr measurement, no other iron-group neutron-rich nucleosynthetic isotope data has been reported for the R chondrites (e.g., Ca, Ti and Ni isotope anomalies). Since the R chondrites are non-carbonaceous chondrites (NCs), studying their ε^{54}Cr composition can also be used to further test, whether the NCs all have different Cr isotopic composition than the carbonaceous chondrites (e.g., Göpel et al., 2015; Sanborn et al., 2019; Trinquier et al., 2007; Warren, 2011).

The variations in the abundance of ^{53}Cr (expressed as ε^{53}Cr) mostly result from the decay of ^{53}Mn, with a half-life of 3.7 Ma (Holden, 1990; Honda and Imamura, 1971). The ^{53}Cr is a sensitive tracer of the timing of formation of the chondrites and their components, and the differentiation of planetesimals and planets (Lugmair and Shukolyukov, 1998; Shukolyukov and Lugmair, 2006). For example, the ^{53}Mn-^{53}Cr short-lived chronometry has been successfully used to date the accretion of chondrite parent bodies (Trinquier et al., 2008) and formation of chondrules (Nyquist et al., 2001; Yamashita et al., 2010; Yin et al., 2007; Yin et al., 2009; Zhu et al., 2019a; Zhu et al., 2020a) of which ages potentially represent the earliest accretion ages of their host chondrites. Therefore, the ε^{53}Cr values of the R chondrites may also provide significant information about the origin of their parent body(ies), as well as its possible relationship to differentiated achondrite parent bodies.

The Cr stable isotopes (expressed as δ^{53}Cr, the per mil variation of the ^{53}Cr/^{52}Cr ratio relative to a terrestrial standard, NIST SRM 979) is a tracer of planetary evolution,

including volatile depletion (Sossi et al., 2018; Zhu et al., 2019c), magmatic processes (Bonnand et al., 2020; Bonnand et al., 2016a; Shen et al., 2019; Sossi et al., 2018; Zhu et al., 2019c), and possibly core formation (Moynier et al., 2011). However, an unknown is the starting isotope composition of the material before fractionation, i.e., those of the planetary precursors. It is therefore important to investigate the presently unknown Cr stable isotopic composition of the R chondrites, including the various petrologic types (from R3 to R6).

Here, we report high-precision mass-independent and mass-dependent Cr isotope data for 12 bulk R chondrites that sample the full range of petrologic types (3-6) and one R chondrite-like clast from a polymict ureilite, Almahata Sitta. We use the radiogenic and nucleosynthetic Cr isotope anomalies and Cr stable isotope compositions of the R chondrites to discuss their possible relationship with other chondrites and achondrites. The Cr isotope composition of the R chondrite-like clast within the polymict ureilite Almahata Sitta (Bischoff et al., 2010; Horstmann and Bischoff 2014) is used to test whether this clast is indeed related to R-chondrites, and further track the potential transport processes and dynamics (from a chondrite parent body to an achondrite parent body) in the early Solar System.

2. Samples and analytical methods

2.1 Sample information and dissolution

The sample suite analyzed in this study includes 12 bulk R chondrites: Rumuruti

(R3.8-6), Pecora Escarpment (PCA) 91002 (R3.8-6), LaPaz Icefield (LAP) 03645 (R), NWA 1476 (R3), NWA 2446 (R3), NWA 753 (R3.9), Miller Range (MIL) 07440 (R4), LAP 03639 (R4), NWA 053 (R4), NWA 6145 (R5), MIL 11207 (R6) and LAP 04840 (R6). We also analyzed one R chondrite-like clast named MS-CH in Almahata Sitta (polymict ureilite). It has previously been described by Horstmann et al. (2010) and reviewed in (Bischoff et al., 2010). In summary, this clast weighs 5.68g, possess ~400 μm chondrules, 40 vol.% of matrix and a $\Delta^{17}O$ value of ~1.7 ‰, which are all similar properties to those of R chondrites. To assess the data quality, we also measured the USGS rock standards DTS-2b, PCC-1 and BHVO-2.

R chondrite samples with no fusion crusts weighing 0.5 to 1 g were crushed to a fine powder using a boron carbide mortar and pestle. A fraction of the powders (ca. 100 mg) were digested by sequential mixtures of concentrated HF+HNO_3 (2:1) and HNO_3 + HCl (1:3) in Parr Bombs under pressurized steel jackets for 3-4 days at 180 °C respectively, and no visible residues were observed. Then, ~1%, ~5% and ~5% aliquots were extracted for measurements of $^{55}Mn/^{52}Cr$ ratios, mass-independent and mass-dependent Cr isotope fractionation, respectively. The rest of the solution is kept for other chemical and isotopic analysis.

2.2 Mass-independent Cr isotope ($\varepsilon^{53}Cr$ and $\varepsilon^{54}Cr$) measurements

A four-step column chemistry was used to purify the sample for mass-independent Cr isotope measurements in a clean laboratory at Earth and Planetary Laboratory, Carnegie Institute for Science. Firstly, we used an anion

chromatographic purification column to efficiently remove Fe and Ni in 6M HCl. Prior to sample loading on cation exchange columns, we used a Cr pre-treatment procedure involving dissolution in 10M HCl at >120 °C to efficiently promote the formation of Cr^{3+}-Cl species, which have a low affinity for the cation exchanger and thus elute early. This was followed by elution of Cr on a 1 ml cation exchange column in 20 ml of 0.5M HNO_3 to remove the major elements, including Mg, Ca, Al, and Ni, and to collect all the Cr species (major Cr^0 and minor Cr^{2+} and Cr^{3+}) to reach a >99% recovery. The samples were then exposed to 0.5M HNO_3 + 0.6% H_2O_2 at room temperature for >1 day to promote the formation of Cr^{3+} (Larsen et al., 2016). However, it is difficult to transform all Cr to Cr^{3+}, so the Cr^0-bearing material is collected in 0.5 ml of the loading solution and 0.5 ml of 0.5N HNO_3 elution to increase the recovery to >95% in the next column. The third clean-up column involved Cr purification from Al, Ti, V, and Fe (and other high-field-strength elements), as well as Na and K, on a small (0.33ml) cation exchange column using 0.5M HNO_3, 1M HF, and 6M HCl. Finally, for the fourth column, 0.7 ml of TODGA resin was used in 8N HCl to remove the residual Fe, V, and Ti (which remained on the column) that have isobaric isotopes with ^{54}Cr (^{54}Fe) and ^{50}Cr (^{50}V and ^{50}Ti) (Pedersen et al., 2019). The full procedure reaches a total yield of between 95% and 99%, and effectively removes any matrix, especially Fe, V, and Ti, that might influence analysis by Multiple Collector-Inductively Coupled Plasma-Mass Spectrometry (MC-ICP-MS). The total blank of the isolation procedure is 10-12 ng for Cr and can be neglected given the typical sample size, ~10 μg of Cr.

The $^{55}Mn/^{52}Cr$ ratios were measured on a MC-ICP-MS Neptune Plus. We initially prepared three Mn-Cr doped artificial standard solutions gravitationally, with Mn–Cr contents of 10–100 ppb, 50–100 ppb and 100–100 ppb and Mn/Cr ratios of 0.1, 0.5 and 1.0. The unpurified sample solutions were diluted to a Cr content of ~100 ppb. The intensities for ^{55}Mn and ^{52}Cr on faraday detectors obtained when analyzing the standard and sample solutions ranged from 0.5 V to 5 V, and 10 cycles of 4 seconds each were measured in each analysis to obtain a target precision for the $^{55}Mn/^{52}Cr$ ratios better than 1%. After establishing a calibration curve ($R^2 > 0.999$) based on the true and measured $^{55}Mn/^{52}Cr$ ratios of the three artificial standards, the $^{55}Mn/^{52}Cr$ ratios of the chondrite samples could be calculated. The final estimated precision is <5% (Zhu et al., 2020a; Zhu et al., 2020b).

Compared to Thermal Ionization Mass Spectrometry (TIMS), chromium isotope analysis by MC-ICP-MS has the advantage that the high ionization efficiency of the plasma results in relative constant mass fractionation, which by use of the sample-standard-bracketing approach can be well corrected for and essentially eliminates the need for consideration of the instrumental mass fractionation. Thermal ionization, on the other hand, inherently does not produce stable mass fractionation through time, which may cause a residual, apparent mass-dependent effect after mass fractionation correction by exponential law (assuming kinetic fractionation), which is demonstrated by the correlation between $\varepsilon^{53}Cr$ and $\varepsilon^{54}Cr$ with slope of ~2.6 of Cr isotope standards (Qin et al., 2010; Trinquier et al., 2006). This effect ultimately limits

199 both the obtainable accuracy and precision of mass fractionation corrected isotope
200 data obtained by TIMS. Therefore, Cr isotope analysis by MC-ICP-MS can achieve
201 higher data precision than by TIMS for comparable measurement signal and time but
202 typically requires larger amount of sample due to the lower transmission efficiency of
203 the MC-ICP-MS (e.g., Pedersen et al., 2019; Schiller et al., 2014; Zhu et al., 2020b).

204 The Cr isotopic compositions of all the samples were determined using one of
205 the MC-ICP-MS Neptune Plus located at the Centre for Star and Planet Formation,
206 Globe Institute, University of Copenhagen. Detailed analytical and data reduction
207 methods are described elsewhere (Pedersen et al., 2019; Schiller et al., 2014; Zhu et
208 al., 2020b). The Cr isotopic composition of each sample was measured by
209 sample-standard bracketing using the NIST SRM 979 Cr standard. Sample solutions
210 with ~0.5 ppm Cr were introduced to the plasma via an ESI Apex IR resulting in ^{52}Cr
211 signals of 20-40 V at an uptake rate of ~0.06 mL/min. Each sample was measured five
212 times and the resulting average 2 standard error (2se) uncertainty for ε^{53}Cr and ε^{54}Cr
213 are ~0.02 and ~0.06, respectively. The ^{53}Cr/^{52}Cr and ^{54}Cr/^{52}Cr ratios were normalized
214 to a constant ^{50}Cr/^{52}Cr ratio of 0.051859 using the exponential law (Lugmair and
215 Shukolyukov, 1998). All the measured isotopic ratios are expressed relative to NIST
216 SRM 979 in the epsilon notations:

217 $$\varepsilon\,{}^{x}Cr \;=\; \left(\frac{\left({}^{x}Cr/{}^{52}Cr\right)_{sample}}{\left({}^{x}Cr/{}^{52}Cr\right)_{NIST\ SRM\ 979}} - 1\right) \times 10000 \quad (1),$$

218 with x = 53 or 54.

2.3 Mass-dependent Cr isotope (δ^{53}Cr) measurements

The whole procedure of mass-dependent Cr isotope analysis was performed at the Institut de Physique du Globe de Paris (IPGP) on aliquots of the same dissolutions used for mass-independent isotope measurements. This measurement techniques followed the same procedure as described in Sossi et al. (2018) and Zhu et al. (2019c). First, the appropriate amount of ^{50}Cr-^{54}Cr double spike (28% of the Cr content endemic to the sample) was added to the aliquot, which was then refluxed in a closed beaker at 120 °C overnight to homogenize the sample and spikes (e.g., Wu et al., 2020). Then, samples were chemically purified for Cr via a two-step cation exchange chromatography followed by previous works (Sossi et al., 2018; Zhu et al., 2019c). This method has a total procedural yield of 60-90% and a blank of ~5 ng of Cr. Compared to the total ~10 µg of Cr, the blank can be neglected. The final Cr cut was evaporated in concentrated HNO_3 drops 3 to 5 times to convert the HCl medium to HNO_3 and to remove leftover organics (i.e., the resin) following which the samples were diluted to a concentration of 1 ppm Cr, in 2% (0.317 M) HNO_3 for isotope analysis.

The Cr stable isotope compositions of these purified samples were measured on a Thermo Scientific Neptune Plus MC-ICP-MS housed at the IPGP. Analytical details are described in Sossi et al. (2018) and Zhu et al. (2019c). The final Cr stable isotope data (δ^{53}Cr) for R chondrites were corrected taking their respective mass-independent

Cr isotope compositions analyzed on the same aliquots. The isotopic ratio for samples is reported in delta notation relative to NIST SRM 979:

$$\delta^{53}Cr(‰) = \left(\frac{(^{53}Cr/^{52}Cr)_{sample}}{(^{53}Cr/^{52}Cr)_{NIST\ SRM\ 979}} - 1\right) \times 1000. \quad (2)$$

The uncertainties quoted for individual samples are 2SD of single sample measurements (100 cycles for at least two times) or 2SD reproducibility of several NIST SRM 979 measurements in the same analytical session (~0.02 ‰), whichever is the largest.

3. Results

All the Mn/Cr ratios, mass-independent and mass-dependent Cr isotope data for the 12 bulk R chondrites and the clast MS-CH from the meteorite/asteroid Almahata Sitta are reported in Table 1. The ε^{54}Cr values for all R chondrites are homogeneous, with an average value of -0.06 ± 0.08 (2SD, N = 12) (Figures 1 and 2). All the R chondrites have a restricted range of ^{55}Mn/^{52}Cr ratios of 0.68 ± 0.04 (2SD, except NWA 2446 which has a ^{55}Mn/^{52}Cr of 0.60), but have different ε^{53}Cr values ranging from 0.19 ± 0.02 to 0.27 ± 0.02 (Figure 3a, b), averaging at 0.23 ± 0.05 (2SD, N = 12). There is no correlation between the ^{55}Mn/^{52}Cr ratios and the ε^{53}Cr values (Figure 3b). The R-chondrite-like clast, MS-CH, possesses ε^{53}Cr = 0.18 ± 0.04 and ε^{54}Cr = -0.16 ± 0.07 that are indistinguishable within uncertainties to those of the R chondrites. Also, all the R chondrites possess homogeneous stable Cr isotope compositions (Figure 4), with an

258 average $\delta^{53}Cr$ = -0.12 ± 0.03 ‰ (2SD, N = 12) that is indistinguishable to that of
259 MS-CH with $\delta^{53}Cr$ of -0.11 ± 0.05 ‰.

260 The mass-independent Cr isotope data for PCC-1 and DTS-2b in this study are
261 consistent with literature data (Qin et al., 2010; Schiller et al., 2014; Trinquier et al.,
262 2007; Trinquier et al., 2008; Zhu et al., 2019b; Zhu et al., 2020b).

263 The mass-dependent $\delta^{53}Cr$ data (measured by double spike technique) for
264 BHVO-2 and PCC-1 are also consistent with the literature data (Bonnand et al., 2016b;
265 Liu et al., 2019; Schoenberg et al., 2016; Sossi et al., 2018; Wu et al., 2020; Zhu et al.,
266 2019c).

267 # 4. Discussion

268 ## 4.1 Homogeneous $\varepsilon^{54}Cr$ in R chondrites

269 Cosmogenic effects, especially in samples with high Fe/Cr ratios and cosmic ray
270 exposure ages (CREA), can modify the Cr isotope composition (e.g., Shima and
271 Honda, 1966). The R chondrites have lower Fe/Cr ratios of ~105 (Kallemeyn et al.,
272 1996; Schulze et al., 1994) and similar CREA of 0.1~74 Ma (Schultz et al., 2005)
273 relative to angrites (Fe/Cr = 70-700; CREA = 6-70 Ma) that do not show any
274 cosmogenic effects (Zhu et al., 2019b). Moreover, the $\varepsilon^{54}Cr$ for all the R chondrites
275 irrespective of their exposure age are indistinguishable from each other, such that the Cr
276 isotope alteration from cosmogenic effects, if present, are currently not detectable and,
277 thus, can be ignored.

As a group/class of NCs, the homogeneous $\varepsilon^{54}Cr$ value of the R chondrites of -0.06 ± 0.08 (2SD, N = 12; Figures 1 and 2) confirms the observation that there is a Cr isotopic difference between the NCs ($\varepsilon^{54}Cr < 0.3$) and the CCs ($\varepsilon^{54}Cr > 0.3$) (Qin et al., 2010; Trinquier et al., 2007). The $\varepsilon^{54}Cr$ values for R chondrites are similar within error to those of the ECs [$\varepsilon^{54}Cr = 0.01 \pm 0.11$; 2SD, N = 12; (Mougel et al., 2018; Qin et al., 2010; Trinquier et al., 2007; Zhu et al., 2020a)]. We can use this new value to update the $\varepsilon^{54}Cr$ sequence between the different groups of chondrites (Figure 1) to be: CC > EC = RC > OC (Göpel et al., 2015; Mougel et al., 2018; Qin et al., 2010; Trinquier et al., 2007). It should be noted that the average $\varepsilon^{54}Cr$ value for R chondrites also overlaps within error with those of the Earth [$\varepsilon^{54}Cr = 0.09 \pm 0.12$; 2SD, N=14, (Mougel et al., 2018; Trinquier et al., 2007)], Moon [$\varepsilon^{54}Cr = 0.09 \pm 0.08$; (Mougel et al., 2018)] and one aubrite meteorite [$\varepsilon^{54}Cr = -0.16 \pm 0.19$; {Trinquier, 2007 #139}]. Other than the $\varepsilon^{54}Cr$ features, the R chondrites also formed with oxygen fugacities [FMQ -4 ~ FMQ 0 oxygen buffer; (Righter and Neff, 2007)] that were much closer to the Earth's upper mantle value [fO_2 = FMQ -4 ~ FMQ +2; (McCammon, 2005)] compared to the much more reduced ECs [FMQ -8 ~ -10; (Righter et al., 2006)] that are more commonly proposed as major building blocks of the Earth (Javoy et al., 2010). However, the R chondrites have much higher $\Delta^{17}O$ values [~2.7 (Bischoff et al., 2011; Schulze et al., 1994; Weisberg et al., 1991)] than the Earth-Moon system [~0; (Cano et al., 2020; Clayton and Mayeda, 1996; Greenwood et al., 2018; Pack and Herwartz, 2014; Wiechert et al., 2001; Young et al., 2016); Figure 2] and the Mg/Si and Al/Si of

299 the R chondrites do not match those of the bulk Earth (Alexander, 2019b). Therefore,
300 while their Cr isotopic composition and oxidation state match the Earth, the R
301 chondrites or their precursors cannot totally represent the building materials for the
302 Earth-Moon system. Nevertheless, in ε^{54}Cr-Δ^{17}O space (Figure 2) the R chondrites
303 define an end member and should, therefore, be considered in mixing models for
304 planetary precursors (e.g., Alexander, 2019a; Alexander, 2019b; Dauphas, 2017). It is
305 also clear that the R chondrites have distinct ε^{54}Cr values from those of the OCs [ε^{54}Cr
306 = -0.39 ± 0.09; (2SD, N = 18; Pedersen et al., 2019; Qin et al., 2010; Trinquier et al.,
307 2007)], suggesting that there is no genetic relationship between them, even though
308 they have some affinities in terms of their bulk compositions (Alexander, 2019b;
309 Kallemeyn et al., 1996; Palme et al., 1996).

310 The CB, CO, and CK chondrites all exhibit ε^{54}Cr variability within each group
311 (Figure 1) and even between several specimens of the same meteorite, e.g., Allende
312 with ε^{54}Cr values ranging from 0.86 ± 0.09 (Trinquier et al., 2007) to 1.10 ± 0.08 (Zhu
313 et al., 2020b). These heterogeneities probably reflect heterogeneities in the
314 abundances of isotopically extreme CAIs, amoeboid olivine aggregates (AOAs) [with
315 high ε^{54}Cr values, up to ~10 (Trinquier et al., 2009)] and chondrules (Bollard et al.,
316 2019; Olsen et al., 2016; Qin et al., 2011; Zhu et al., 2019a; Zhu et al., 2020a) at the
317 scale of the samples analyzed. All measured R chondrites have similar ε^{54}Cr values,
318 which is consistent with the very low CAI abundances in R chondrites (Russell, 1998).
319 Similar to the CK chondrites, OCs, and ECs that also experienced various degrees of

metamorphism, with petrological types of 3~6 (Pedersen et al., 2019; Qin et al., 2010; Trinquier et al., 2007), the ε^{54}Cr values of the RCs are independent of petrologic types. This confirms that metamorphism on chondrite parent bodies did not cause the loss of ^{54}Cr-rich carrying phases (e.g., Dauphas et al., 2010; Nittler et al., 2018; Qin et al., 2011).

4.2 The ^{53}Mn-^{53}Cr systematics in R chondrites.

It can be seen in Figure 3 that the R chondrites have almost uniform ^{55}Mn/^{52}Cr ratios (averagely ~0.68) but variable ε^{53}Cr values. The ε^{53}Cr variation within the R chondrite parent body should result from the mixing of their chondritic components. Chondrites are complex assemblages, including CAIs, AOAs, chondrules, metals, sulfides, and matrix, and these different components formed at different times and under varying physical conditions (Krot et al., 2014). Refractory inclusions are scarce in R chondrites, i.e., CAIs + AOAs that are < 0.1 vol.% (Bischoff et al., 2011; Krot et al., 2014), so the mixing of different proportion for chondrules and matrix may contribute to the ε^{53}Cr variations. Chondrules are high-temperature magmatic objects and they or their precursors experienced volatile element fractionation (Mahan et al., 2018; Palme et al., 2014; Pringle et al., 2017) that caused Mn/Cr variability. Chondrules' redox history evolved with time, but globally they are reduced and probably formed at fO_2 of iron–wüstite buffer (IW) -1 to -2 (Mahan et al., 2018), under which conditions Mn is more volatile than Cr (Sossi et al., 2019). This explains why chondrules have on average lower Mn/Cr ratios [e.g., CO chondrules with

$^{55}Mn/^{52}Cr$ ranging from 0.2-0.7; (Zhu et al., 2019a)] than unfractionated matrix that can be represented by CI chondrites with $^{55}Mn/^{52}Cr$ of ~0.8 (Qin et al., 2010; Trinquier et al., 2008) and on average lower $\varepsilon^{53}Cr$ [e.g., CO chondrules with $\varepsilon^{53}Cr$ ranging from 0.0 to 0.2; (Zhu et al., 2019a)] than matrix representing by CI chondrites with $\varepsilon^{53}Cr$ of 0.20-0.25 (Qin et al., 2010; Trinquier et al., 2008). The bulk R chondrites, OCs and ECs all have similar Mn/Cr ratios, but the $\varepsilon^{53}Cr$ values of OCs and ECs are systematically lower than those of the R chondrite (Figure 3). This $\varepsilon^{53}Cr$ difference between different chondrite groups may simply reflect the different $\varepsilon^{53}Cr$ reservoirs in different chondrite accretion regions.

4.3 Homogeneous $\delta^{53}Cr$ in R chondrites.

Previous studies have shown that all the CCs, OCs, and ECs have homogeneous Cr stable isotope compositions, $\delta^{53}Cr = -0.11 \pm 0.05$ ‰ [2SD, N = 30; $N_{CC} = 11$, $N_{OC} = 17$, $N_{EC} = 2$; (Bonnand et al., 2016b; Schoenberg et al., 2016)]. The $\delta^{53}Cr$ values for all chondrites are similar to that of the bulk silicate Earth [$\delta^{53}Cr = -0.11 \pm 0.06$ ‰; 2SD, N = 36; (Schoenberg et al., 2008; Sossi et al., 2018)], suggesting that core formation or volatile processes cause little Cr stable isotope fractionation, which is further supported by high-pressure metal-silicate experiments (Bonnand et al., 2016b). In this study, we found that the $\delta^{53}Cr$ values for the R chondrites, -0.12 ± 0.03 ‰ (2SD, N = 12), also fall in the chondrite-Earth $\delta^{53}Cr$ range. This supports the view that, when corrected for their different nucleosynthetic signatures, the chondrite reservoirs have a homogeneous Cr stable isotope with $\delta^{53}Cr = -0.12 \pm 0.04$ ‰ (2SD, N =42).

Different chondrites groups record different redox conditions (Rubin et al., 1988). In detail, the oxidized R and CV_{oxi} chondrites record oxygen fugacities (fO_2) of fayalite-magnetite-quartz buffer (FMQ) ~-2, OCs have fO_2 of FMQ ~-6, and ECs are the most reduced, with fO_2 of FMQ -8 to -10 (Righter et al., 2006; Righter and Neff, 2007). The varied redox conditions for different chondrite groups correlate with their hydrogen isotope ratios (Alexander, 2019b), suggesting that the addition of water plays an important role in oxidation. The Cr stable isotope compositions of all these chondrites are homogeneous and, therefore, were not affected by parent body fO_2 conditions. This is perhaps surprising given the resolvable isotopic fractionation observed during Cr^{2+}/Cr^{3+} exchange in magmatic processes on the Earth (Bonnand et al., 2020; Shen et al., 2019), the Moon (Bonnand et al., 2016a; Sossi et al., 2018) and HEDs [(perhaps Vesta; (Zhu et al., 2019c)). However, it is firstly consistent with that water contained little Cr, which would not change the Cr species in chondrite parent body. Then, although it is possible that the presence of water oxidized Cr from Cr^{2+} to Cr^{3+}, which may result in Cr stable isotope fractionation (Cr^{3+} would be isotopically heavier than Cr^{2+}). However, in absence of loss of Cr via volatilization from the chondrite parent body, this effect would not lead to Cr isotope fractionation between chondrite groups. In any case, the homogeneous $\delta^{53}Cr$ values between all chondrite groups strongly suggests that differentiated planets also had initial $\delta^{53}Cr$ similar to chondrites, since chondrites are believed as their precursors (e.g., Allègre et al., 1995). The Cr stable isotopic difference between planetary mantles with different oxygen

fugacities, e.g., Earth [δ^{53}Cr = -0.11 ± 0.06 (Schoenberg et al., 2008; Sossi et al., 2018)], Moon [δ^{53}Cr = -0.21 ± 0.03 (Bonnand et al., 2016a; Sossi et al., 2018)] and HEDs (Vesta) [δ^{53}Cr = -0.22 ± 0.03 (Zhu et al., 2019c)], is not due to variability in the initial composition but to planetary differentiation processes, e.g., volatile depletion and/or partial melting (Sossi et al., 2018; Zhu et al., 2019c).

The R chondrites with petrologic types ranging from 3 to 6 have homogeneous δ^{53}Cr values, suggesting that metamorphism does not affect the Cr isotopic composition of the bulk samples. In detail, metamorphism would not redistribute the Cr species inside chondrite parent bodies, which mimics the water effect as discussed above. Thus, in consequence, no differences were observed studying the Cr isotopic compositions of the brecciated rocks among the R chondrites. This is also consistent with the lack of resolvable Cr stable isotopic variability among metamorphic rocks (Shen et al., 2015; Wang et al., 2016), the δ^{53}Cr value of every R chondrite can represent its bulk parent body.

4.4 Chromium isotope composition of the R chondrite-like clast of Almahata Sitta

Almahata Sitta (debris from asteroid 2008 TC3) is a polymict ureilite that contains not only ureilitic clasts but also some chondritic clasts from OCs and ECs (Bischoff et al., 2010). One of the chondritic clasts, MS-CH, is unusual. It is a petrologic type ~3.8 chondrite with a chondrule/matrix ratio of about 1.5. This clast has a Δ^{17}O = ~1.76 and contains chondrules with an average size of roughly 450 μm

404 (Horstmann et al., 2010). All these characteristics are similar to those of the R
405 chondrites. The $^{55}Mn/^{52}Cr$, $\varepsilon^{53}Cr$ and $\varepsilon^{54}Cr$ values for this clast determined here are
406 0.70 ± 0.04, 0.18 ± 0.04, and -0.16 ± 0.07, respectively, and also resemble those of R
407 chondrites [$^{55}Mn/^{52}Cr$ = 0.68 ± 0.04, $\varepsilon^{53}Cr$ = 0.23 ± 0.05, and $\varepsilon^{54}Cr$ = -0.06 ± 0.08
408 (2SD, N = 12)]. These compositions also support the classification of this clast as R
409 chondrite-like. It should be noted that this clast cannot have any genetic relationship
410 to CK chondrites, which have higher $\varepsilon^{54}Cr$ ranging from 0.33 ± 0.12 (Qin et al., 2010)
411 to 0.63 ± 0.09 (Trinquier et al., 2007), although the clast contains equilibrated and
412 metamorphosed olivine, similar to CK chondrites (Horstmann et al., 2010). The $\delta^{53}Cr$
413 value of this clast (-0.11 ± 0.15) is also consistent with that of R chondrites, but since
414 all chondrites have similar stable isotopic composition, this is not surprising. However,
415 it should be noted that both the $\Delta^{17}O$ and $\varepsilon^{54}Cr$ values for this clast are slightly lower
416 than those of the R chondrite group. More importantly, the clast contains some metals
417 (unknown from R chondrites) and chromites in this clast have much lower TiO_2
418 (~1.35 wt.%) contents (Horstmann et al., 2010) than those of R chondrites
419 (typically >5 wt.%; (Bischoff et al., 2011). There are also no magnetites and
420 platinum-group-element-rich phases in this clast, while this is usually the case for R
421 chondrites (Horstmann et al., 2010). Therefore, the chemical, petrological and
422 isotopic features of this clast do not match any currently known chondrite groups and
423 it should remain an ungrouped non-carbonaceous chondrite. The similar $\Delta^{17}O$ and
424 $\varepsilon^{54}Cr$ signatures between this clast and the R chondrites may suggest they accreted at

425 a similar locations or in a similar environments in the Solar System (e.g., Desch et al.,
426 2018). Furthermore, the observation of chondritic clasts in achondrites (e.g., Zolensky
427 et al., 1996; Goodrich et al., Bischoff et al., 2006; 2010; Patzek et al., 2018) is
428 consistent with the extensive transportation processes in early Solar System
429 (Weidenschilling, 1977), which is also supported by the transportation of chondrule
430 precursors (Olsen et al., 2016; Zhu et al., 2019a; Zhu et al., 2020a) and the
431 observation of an angrite-like clast in a CH chondrite (Zhang et al., 2020).
432

5. Conclusion

This work reports the first high-precision nucleosynthetic signatures of the Rumuruti (R) chondrites. All the R chondrites possess homogeneous ε^{54}Cr: -0.06 ± 0.08 (2SD, N = 12), which is independent on their petrological types (R3-R6). The ε^{54}Cr values for R chondrites are similar to those of enstatite chondrites, the Earth-Moon system, and aubrites.

R chondrites have ^{55}Mn/^{52}Cr of ~0.68 and ε^{53}Cr of 0.23 ± 0.05 (2SD, N = 12), which are higher than those of most of other chondrite groups. The variable ^{55}Mn/^{52}Cr and ε^{53}Cr may be caused by the different abundance of chondrules that experienced volatile-loss and are, on average, depleted in Mn.

All the R chondrites with types of 3-6 (as well as brecciated R chondrites) possess homogeneous δ^{53}Cr values, -0.12 ± 0.03 (2SD, N = 12). This clearly indicates that metamorphism on chondrite parent bodies does not fractionate Cr stable isotopes. Combined with other chondrites, all the chondrites define a homogeneous δ^{53}Cr = -0.12 ± 0.04 (2SD, N = 40). The δ^{53}Cr homogeneity between chondrites and Earth confirms that terrestrial core formation and/or any volatilization did not cause Cr stable isotope fractionation.

Finally, the chondritic clast, MS-CH, within the Almahata Sitta polymict ureilite has ε^{53}Cr = 0.18 ± 0.04, ε^{54}Cr = -0.16 ± 0.07, and δ^{53}Cr = -0.11 ± 0.05 reinforcing its close affinity to R-chondrites, although other chemical and petrological evidence does

not support it to be a clast from the R chondrite parent body.

Acknowledgements

Three reviewers, Associate Editor Yuri Amelin and Executive Editor Jeffrey G. Catalano are deeply thanked for constructive comments which greatly improved the quality of this paper. We thank the Meteorite Working Group (NASA), and the Museum für Naturkunde (Berlin; A. Greshake) for providing additional samples of Rumuruti chondrites. US Antarctic meteorite samples are recovered by the Antarctic search for Meteorites (ANSMET) program which has been funded by NSF and NASA, and characterized and curated in the Department of Mineral Sciences of the Smithsonian Institution and Astromaterials Curation Office at NASA Johnson Space Center. F. M. acknowledges funding from the European Research Council under the H2020 framework program/ERC grant agreement (ERC starting grant, #637503-PRISTINE) and financial support of the UnivEarthS Labex program at Sorbonne Paris Cité (#ANR-10-LABX-0023 and #ANR-11-IDEX-0005-02), and the ANR through a chaire d'excellence Sorbonne Paris Cité. M. S. acknowledges funding from the Villum Fonden (#00025333). M. B. acknowledges funding from the Carlsberg Foundation (#CF18-1105), the Danish National Research Foundation (#DNRF97) and the European Research Council (ERC Advanced Grant Agreement, #833275-DEEPTIME). A. B. thanks the support by the Deutsche Forschungsgemeinschaft (DFG, German Research Foundation, #263649064) – TRR 170 (subproject B05). This is TRR170 Publication No. xx. K. Z. thanks the China Scholarship Council (CSC) for the PhD

475 fellowship (#201706340161) and IPGP for the funding support of traveling, “Aide à la
476 MOBILITE INTERNATIONALE des doctorants de l’IPGP (2019)”, to visit Carnegie
477 Science. Timothy Mock and Mary Horan are appreciated for their assistance in ICP-MS
478 analysis and clean labs respectively.

Table 1 The ^{53}Mn-^{53}Cr and Cr stable isotope data for Rumuruti (R) chondrites, one R chondrite-like clast in a polymict ureilite (Almahata Sitta) and other data quality-control standards.

Name	Type	^{55}Mn/^{52}Cr	ε^{53}Cr	2SE	ε^{54}Cr	2SE	N	δ^{53}Cr	2SD	N
Rumuruti	R3.8-6	0.71	**0.27**	0.03	**-0.03**	0.04	5	**-0.11**	0.02	2
PCA 91002	R3.8-6	0.68	**0.25**	0.01	**-0.05**	0.07	5	**-0.12**	0.04	2
LAP 03645	R	0.69	**0.20**	0.02	**-0.01**	0.04	5	**-0.14**	0.02	2
NWA 1476	R3	0.73	**0.23**	0.02	**-0.10**	0.06	5	**-0.11**	0.02	2
NWA 2446	R3	0.60	**0.20**	0.04	**-0.12**	0.05	5	**-0.11**	0.03	2
NWA 753	R3.9	0.66	**0.22**	0.02	**-0.06**	0.06	5	**-0.09**	0.03	2
MIL 07440	R4	0.69	**0.25**	0.03	**-0.06**	0.07	5	**-0.13**	0.04	3
LAP 03639	R4	0.68	**0.24**	0.01	**-0.01**	0.06	5	**-0.13**	0.03	2
NWA 053	R4	0.66	**0.27**	0.02	**-0.13**	0.03	5	**-0.11**	0.03	2
NWA 6145	R5	0.67	**0.22**	0.02	**-0.07**	0.10	5	**-0.12**	0.02	2
MIL 11207	R6	0.69	**0.19**	0.02	**-0.04**	0.07	5	**-0.12**	0.03	2
LAP 04840	R6	0.68	**0.22**	0.02	**-0.03**	0.03	5	**-0.12**	0.02	2
MS-CH	Clast in Ureilite	0.70	**0.18**	0.04	**-0.16**	0.07	5	**-0.11**	0.05	4
BHVO-2	Basalt							**-0.11**	0.03	2
PCC-1	Peridotite		**-0.02**	0.03	**0.01**	0.07	5	**-0.08**	0.05	4
DTS-2b	Dunite		**0.06**	0.02	**0.12**	0.06	5			

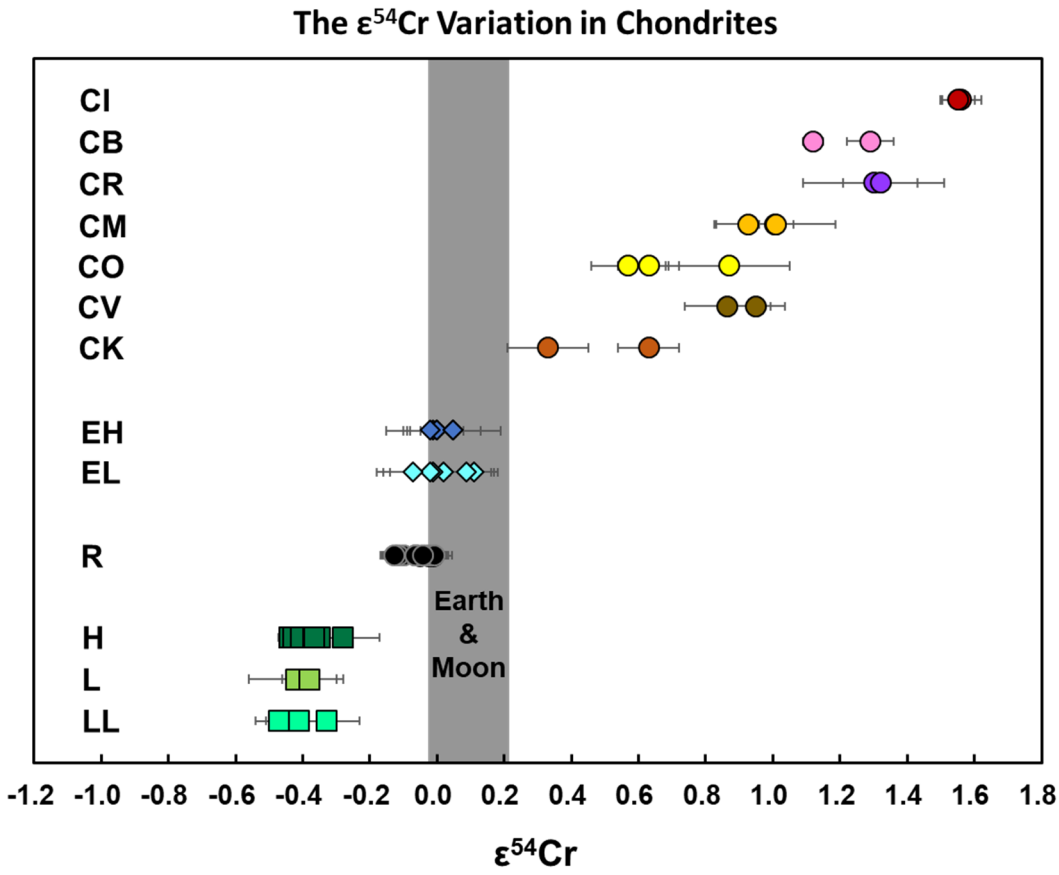

Figure 1 The $\varepsilon^{54}Cr$ variation for different groups of chondrites. The warm-color circles are the carbonaceous chondrites that all possess $\varepsilon^{54}Cr > 0.3$, while the blue diamonds, black circles, and green squares indicate the enstatite (EH, EL), Rumuruti, and ordinary (H, L, LL) chondrites, respectively. The gray bar indicates the $\varepsilon^{54}Cr$ values for the Earth-Moon system. The data for the Rumuruti chondrites are from this study, and the others come from the literature data (Göpel et al., 2015; Mougel et al., 2018; Pedersen et al., 2019; Qin et al., 2010; Trinquier et al., 2007; Trinquier et al., 2008; Yamashita et al., 2010). The $\varepsilon^{54}Cr = 0.09 \pm 0.12$ (2SD, N = 14) for Earth is from data in this study and literature (Mougel et al., 2018; Trinquier et al., 2007), while the $\varepsilon^{54}Cr = 0.09 \pm 0.08$ for the Moon is from Mougel et al. (2018).

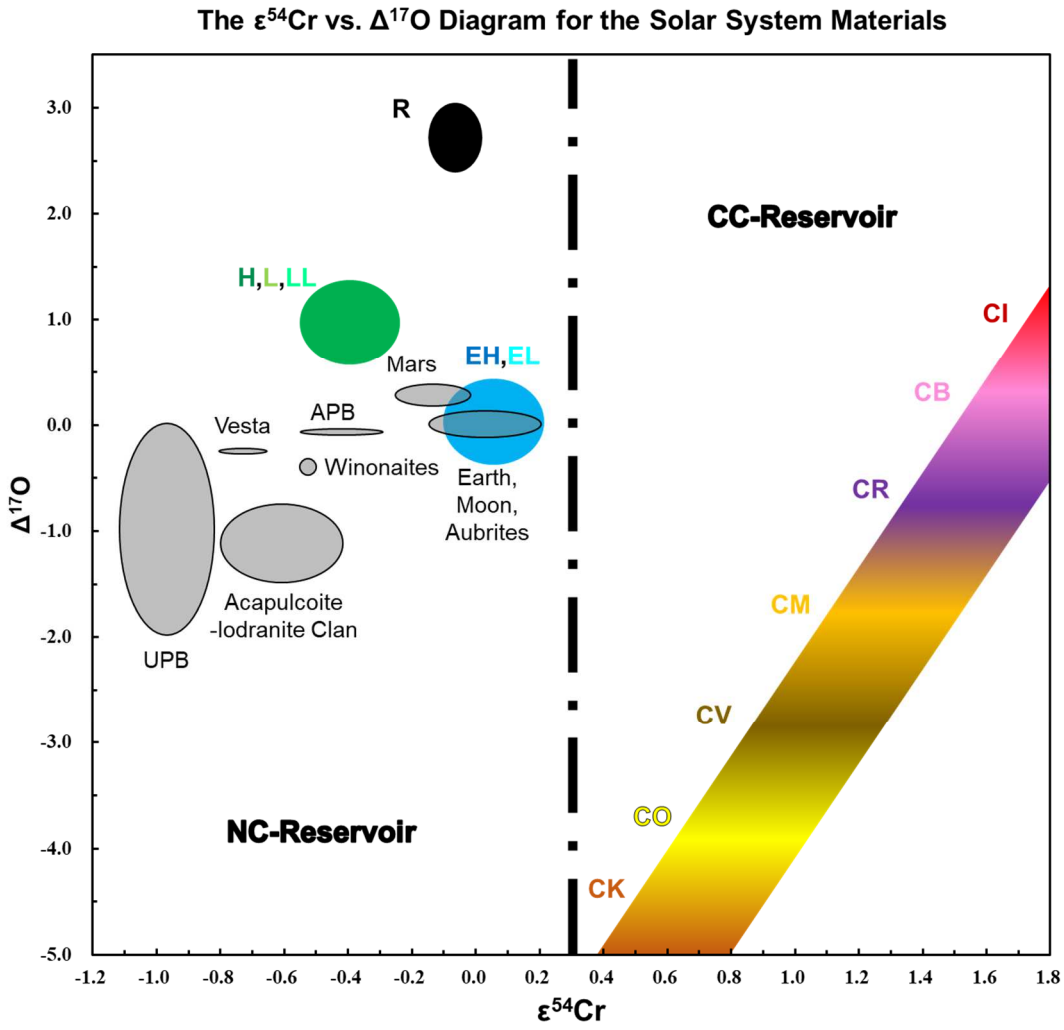

493

494 Figure 2. The $\varepsilon^{54}Cr$ and $\Delta^{17}O$ values of CCs (warm-color shade), OCs (green shade), ECs (blue shade),
495 and RCs (black shade), as well as achondrites, terrestrial and lunar samples (gray ellipses). The $\varepsilon^{54}Cr$
496 and $\Delta^{17}O$ values are positively correlated in CCs, e.g., CK chondrites have the lowest $\varepsilon^{54}Cr$ and $\Delta^{17}O$
497 values, while CI chondrites have the highest $\varepsilon^{54}Cr$ and $\Delta^{17}O$ values (Clayton and Mayeda, 1999;
498 Trinquier et al., 2007). The R chondrites (described as average values with 2SD uncertainty) are
499 located at the top of this diagram. CC: Carbonaceous chondrite; NC: non-CCs; APB: angrite parent
500 body; UPB: ureilite parent body. The colored circles represent the same samples in Fig. 1. The detailed
501 data source for Cr isotopes are: chondrites (Göpel et al., 2015; Mougel et al., 2018; Qin et al.,
502 2010; Trinquier et al., 2007), Earth (Qin et al., 2010; Trinquier et al., 2007), Moon (Mougel et al.,
503 2018), one aubrite (Trinquier et al., 2007), SNC-Mars (Kruijer et al., 2020), angrite APB (Zhu et
504 al., 2019b), HED-Vesta (Trinquier et al., 2007), Acapulcoite-Lodranite clan (Li et al., 2018),
505 Winonaites (Li et al., 2018), UPB (Yamakawa et al., 2010; Zhu et al., 2020b). The O isotope data
506 sources are from two review papers (Greenwood et al., 2017; Ireland et al., 2020).
507
508

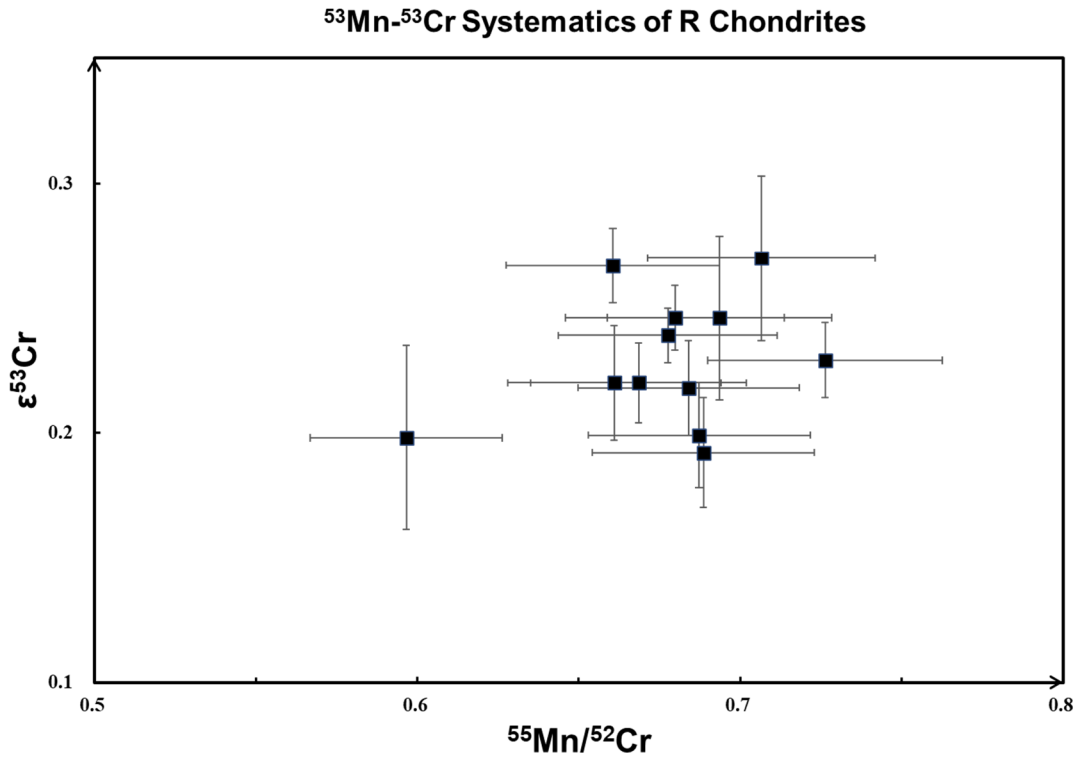

509

510 Figure 3 The ^{53}Mn-^{53}Cr data of R chondrites. Most of R chondrite have similar ^{55}Mn/^{52}Cr ratios
511 (~0.68) but distinguishable ε^{53}Cr values, which may be caused by the variable abundance of
512 chondrules and matrix.

513

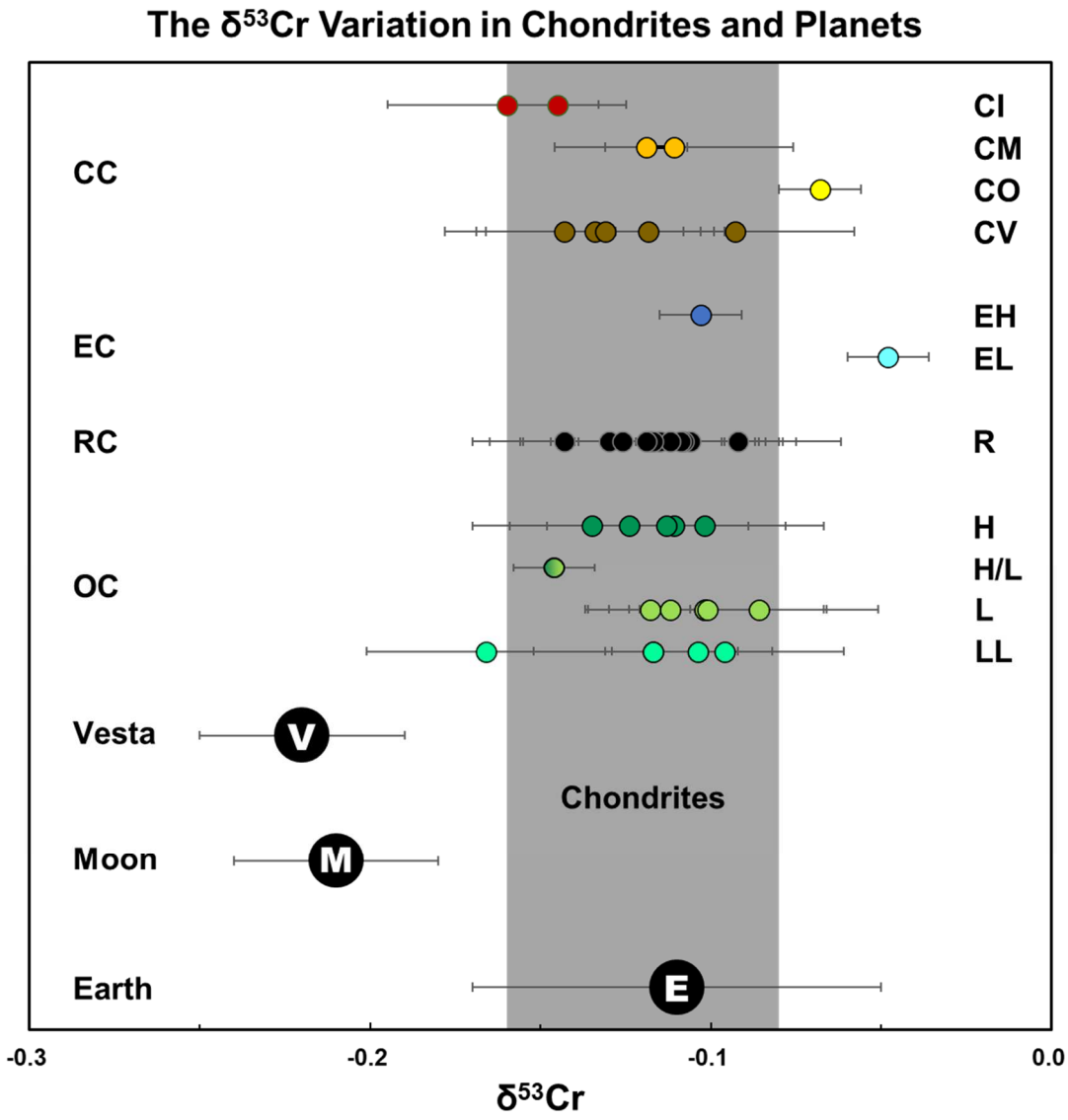

514

515 Figure 4. Comparison of the $\delta^{53}Cr$ variations amongst chondrites, achondrites and the Earth-Moon
516 system. The circles are chondrites of which color corresponds to Figure 1, 2 and 3, while the real
517 pictures of planets represent the Earth, Moon and Vesta themselves. The gray bar defines the
518 average $\delta^{53}Cr$ values (-0.12 ± 0.04; 2SD, N =42) of all the chondrites. Literature data sources:
519 chondrites (Bonnand et al., 2016b; Schoenberg et al., 2016), Earth (Jerram et al., 2020;
520 Schoenberg et al., 2008; Sossi et al., 2018), Moon (Bonnand et al., 2016a; Sossi et al., 2018) and
521 HEDs-Vesta (Zhu et al., 2019c).

522

ReferencesMeteoritical Bulletin.
Alexander, C.M.O.D. (2019a) Quantitative models for the elemental and isotopic fractionations in chondrites: The carbonaceous chondrites. Geochimica et Cosmochimica Acta 254, 277-309.
Alexander, C.M.O.D. (2019b) Quantitative models for the elemental and isotopic fractionations in the non-carbonaceous chondrites. Geochimica et Cosmochimica Acta 254, 246-276.
Allègre, C.J., Poirier, J.-P., Humler, E. and Hofmann, A.W. (1995) The chemical composition of the Earth. Earth and Planetary Science Letters 134, 515-526.
Bischoff, A., Geiger, T., Palme, H., Spettel, B., Schultz, L., Scherer, P., Loeken, T., Bland, P., Clayton, R. and Mayeda, T. (1994) Acfer 217-A new member of the Rumuruti chondrite group (R). Meteoritics 29, 264-274.
Bischoff, A., Horstmann, M., Pack, A., Laubenstein, M. and Haberer, S. (2010) Asteroid 2008 TC3—Almahata Sitta: A spectacular breccia containing many different ureilitic and chondritic lithologies. Meteoritics & Planetary Science 45, 1638-1656.
Bischoff, A., Vogel, N. and Roszjar, J. (2011) The Rumuruti chondrite group. Geochemistry 71, 101-133.
Bollard, J., Kawasaki, N., Sakamoto, N., Olsen, M., Itoh, S., Larsen, K., Wielandt, D., Schiller, M., Connelly, J.N., Yurimoto, H. and Bizzarro, M. (2019) Combined U-corrected Pb-Pb dating and 26Al-26Mg systematics of individual chondrules – Evidence for a reduced initial abundance of 26Al amongst inner Solar System chondrules. Geochimica et Cosmochimica Acta 260, 62-83.
Bonnand, P., Doucelance, R., Boyet, M., Bachèlery, P., Bosq, C., Auclair, D. and Schiano, P. (2020) The influence of igneous processes on the chromium isotopic compositions of Ocean Island basalts. Earth and Planetary Science Letters 532, 116028.
Bonnand, P., Parkinson, I.J. and Anand, M. (2016a) Mass dependent fractionation of stable chromium isotopes in mare basalts: Implications for the formation and the differentiation of the Moon. Geochimica et Cosmochimica Acta 175, 208-221.
Bonnand, P., Williams, H.M., Parkinson, I.J., Wood, B.J. and Halliday, A.N. (2016b) Stable chromium isotopic composition of meteorites and metal–silicate experiments: Implications for fractionation during core formation. Earth and Planetary Science Letters 435, 14-21.
Cano, E.J., Sharp, Z.D. and Shearer, C.K. (2020) Distinct oxygen isotope compositions of the Earth and Moon. Nature Geoscience, 1-5.
Clayton, R.N. and Mayeda, T.K. (1996) Oxygen isotope studies of achondrites. Geochimica et Cosmochimica Acta 60, 1999-2017.
Clayton, R.N. and Mayeda, T.K. (1999) Oxygen isotope studies of carbonaceous chondrites. Geochimica et Cosmochimica Acta 63, 2089-2104.
Dauphas, N. (2017) The isotopic nature of the Earth's accreting material through time. Nature 541, 521.
Dauphas, N., Remusat, L., Chen, J., Roskosz, M., Papanastassiou, D., Stodolna, J., Guan, Y., Ma, C. and Eiler, J. (2010) Neutron-rich chromium isotope anomalies in

565 supernova nanoparticles. The Astrophysical Journal 720, 1577.
566 Desch, S.J., Kalyaan, A. and Alexander, C.M.D. (2018) The effect of Jupiter's
567 formation on the distribution of refractory elements and inclusions in meteorites. The
568 Astrophysical Journal Supplement Series 238, 11.
569 Göpel, C., Birck, J.-L., Galy, A., Barrat, J.-A. and Zanda, B. (2015) Mn–Cr systematics
570 in primitive meteorites: Insights from mineral separation and partial dissolution.
571 Geochimica et Cosmochimica Acta 156, 1-24.
572 Greenwood, R.C., Barrat, J.-A., Miller, M.F., Anand, M., Dauphas, N., Franchi, I.A.,
573 Sillard, P. and Starkey, N.A. (2018) Oxygen isotopic evidence for accretion of Earth's
574 water before a high-energy Moon-forming giant impact. Science advances 4, eaao5928.
575 Greenwood, R.C., Burbine, T.H., Miller, M.F. and Franchi, I.A. (2017) Melting and
576 differentiation of early-formed asteroids: The perspective from high precision oxygen
577 isotope studies. Chemie der Erde 77, 1-43.
578 Holden, N.E. (1990) Total half-lives for selected nuclides. Pure and Applied Chemistry
579 62, 941-958.
580 Honda, M. and Imamura, M. (1971) Half-life of Mn 53. Physical Review C 4,
581 1182-1188.
582 Horstmann, M., Bischoff, A., Pack, A. and Laubenstein, M. (2010) Almahata
583 Sitta—Fragment MS-CH: Characterization of a new chondrite type. Meteoritics &
584 Planetary Science 45, 1657-1667.
585 Ireland, T.R., Avila, J., Greenwood, R.C., Hicks, L.J. and Bridges, J.C. (2020) Oxygen
586 Isotopes and Sampling of the Solar System. Space Science Reviews 216, 25.
587 Javoy, M., Kaminski, E., Guyot, F., Andrault, D., Sanloup, C., Moreira, M., Labrosse,
588 S., Jambon, A., Agrinier, P. and Davaille, A. (2010) The chemical composition of the
589 Earth: Enstatite chondrite models. Earth and Planetary Science Letters 293, 259-268.
590 Jerram, M., Bonnand, P., Kerr, A.C., Nisbet, E.G., Puchtel, I.S. and Halliday, A.N.
591 (2020) The δ53Cr isotope composition of komatiite flows and implications for the
592 composition of the bulk silicate Earth. Chemical Geology 551, 119761.
593 Kallemeyn, G.W., Rubin, A.E. and Wasson, J.T. (1996) The compositional
594 classification of chondrites: VII. The R chondrite group. Geochimica et Cosmochimica
595 Acta 60, 2243-2256.
596 Krot, A.N., Keil, K., Scott, E.R.D., Goodrich, C.A. and Weisberg, M.K. (2014) 1.1 -
597 Classification of Meteorites and Their Genetic Relationships A2 - Holland, Heinrich D,
598 in: Turekian, K.K. (Ed.), Treatise on Geochemistry (Second Edition). Elsevier, Oxford,
599 pp. 1-63.
600 Kruijer, T.S., Borg, L.E., Wimpenny, J. and Sio, C.K. (2020) Onset of magma ocean
601 solidification on Mars inferred from Mn-Cr chronometry. Earth and Planetary Science
602 Letters, 116315.
603 Larsen, K.K., Trinquier, A., Paton, C., Schiller, M., Wielandt, D., Ivanova, M.A.,
604 Connelly, J.N., Nordlund, Å., Krot, A.N. and Bizzarro, M. (2011) Evidence for
605 magnesium isotope heterogeneity in the solar protoplanetary disk. The Astrophysical
606 Journal Letters 735, L37.

607 Larsen, K.K., Wielandt, D., Schiller, M. and Bizzarro, M. (2016) Chromatographic
608 speciation of Cr(III)-species, inter-species equilibrium isotope fractionation and
609 improved chemical purification strategies for high-precision isotope analysis. Journal
610 of Chromatography A 1443, 162-174.
611 Li, S., Yin, Q.-Z., Bao, H., Sanborn, M.E., Irving, A., Ziegler, K., Agee, C., Marti, K.,
612 Miao, B., Li, X., Li, Y. and Wang, S. (2018) Evidence for a multilayered internal
613 structure of the chondritic acapulcoite-lodranite parent asteroid. Geochimica et
614 Cosmochimica Acta 242, 82-101.
615 Liu, C.Y., Xu, L.J., Liu, C.T., Liu, J., Qin, L.P., Zhang, Z.D., Liu, S.A. and Li, S.G.
616 (2019) High-Precision Measurement of Stable Cr Isotopes in Geological Reference
617 Materials by a Double-Spike TIMS Method. Geostandards and Geoanalytical Research
618 43, 647-661.
619 Lugmair, G. and Shukolyukov, A. (1998) Early solar system timescales according to 53
620 Mn-53 Cr systematics. Geochimica et Cosmochimica Acta 62, 2863-2886.
621 Mahan, B., Moynier, F., Siebert, J., Gueguen, B., Agranier, A., Pringle, E.A., Bollard, J.,
622 Connelly, J.N. and Bizzarro, M. (2018) Volatile element evolution of chondrules
623 through time. Proceedings of the National Academy of Sciences, 201807263.
624 McCammon, C. (2005) The paradox of mantle redox. Science 308, 807-808.
625 Mougel, B., Moynier, F. and Göpel, C. (2018) Chromium isotopic homogeneity
626 between the Moon, the Earth, and enstatite chondrites. Earth and Planetary Science
627 Letters 481, 1-8.
628 Moynier, F., Yin, Q.-Z. and Schauble, E. (2011) Isotopic evidence of Cr partitioning
629 into Earth's core. Science 331, 1417-1420.
630 Nittler, L.R., Alexander, C.M.D., Liu, N. and Wang, J. (2018) Extremely 54Cr-and
631 50Ti-rich Presolar Oxide Grains in a Primitive Meteorite: Formation in Rare Types of
632 Supernovae and Implications for the Astrophysical Context of Solar System Birth. The
633 Astrophysical Journal Letters 856, L24.
634 Nyquist, L., Lindstrom, D., Mittlefehldt, D., SHIH, C.Y., Wiesmann, H., Wentworth, S.
635 and Martinez, R. (2001) Manganese-chromium formation intervals for chondrules from
636 the Bishunpur and Chainpur meteorites. Meteoritics & Planetary Science 36, 911-938.
637 Olsen, M.B., Wielandt, D., Schiller, M., Van Kooten, E.M.M.E. and Bizzarro, M. (2016)
638 Magnesium and 54Cr isotope compositions of carbonaceous chondrite chondrules –
639 Insights into early disk processes. Geochimica et Cosmochimica Acta 191, 118-138.
640 Pack, A. and Herwartz, D. (2014) The triple oxygen isotope composition of the Earth
641 mantle and understanding ΔO17 variations in terrestrial rocks and minerals. Earth and
642 Planetary Science Letters 390, 138-145.
643 Palme, H., Lodders, K. and Jones, A. (2014) 2.2 - Solar System Abundances of the
644 Elements, in: Holland, H.D., Turekian, K.K. (Eds.), Treatise on Geochemistry (Second
645 Edition). Elsevier, Oxford, pp. 15-36.
646 Palme, H., Weckwerth, G. and Wolf, D. (1996) The composition of a new R-chondrite
647 and the classification of chondritic meteorites, Lunar and Planetary Science
648 Conference.

649 Pedersen, S.G., Schiller, M., Connelly, J.N. and Bizzarro, M. (2019) Testing accretion
650 mechanisms of the H chondrite parent body utilizing nucleosynthetic anomalies.
651 Meteoritics & Planetary Science 54, 1215-1227.
652 Pringle, E.A., Moynier, F., Beck, P., Paniello, R. and Hezel, D.C. (2017) The origin of
653 volatile element depletion in early solar system material: Clues from Zn isotopes in
654 chondrules. Earth and Planetary Science Letters 468, 62-71.
655 Qin, L., Alexander, C.M.O.D., Carlson, R.W., Horan, M.F. and Yokoyama, T. (2010)
656 Contributors to chromium isotope variation of meteorites. Geochimica et
657 Cosmochimica Acta 74, 1122-1145.
658 Qin, L., Nittler, L.R., Alexander, C.M.O.D., Wang, J., Stadermann, F.J. and Carlson,
659 R.W. (2011) Extreme 54Cr-rich nano-oxides in the CI chondrite Orgueil – Implication
660 for a late supernova injection into the solar system. Geochimica et Cosmochimica Acta
661 75, 629-644.
662 Righter, K., Drake, M.J. and Scott, E. (2006) Compositional relationships between
663 meteorites and terrestrial planets. Meteorites and the early solar system II 943, 803-828.
664 Righter, K. and Neff, K. (2007) Temperature and oxygen fugacity constraints on CK
665 and R chondrites and implications for water and oxidation in the early solar system.
666 Polar Science 1, 25-44.
667 Rubin, A.E., Fegley, B. and Brett, R. (1988) Oxidation state in chondrites, in: Kerridge,
668 J.F., Matthews, M.S. (Eds.), Meteorites and the Early Solar System. University of
669 Arizona Press, Tucson, Arizona, pp. 488-511.
670 Rubin, A.E. and Kallemeyn, G.W. (1994) Pecora Escarpment 91002: A member of the
671 new Rumuruti (R) chondrite group. Meteoritics 29, 255-264.
672 Russell, S. (1998) A Survey of Calcium-Aluminum-rich Inclusions from R Chondrites:
673 Implications for Relationships Between Meteorite Groups. Meteoritics and Planetary
674 Science Supplement 33, A131.
675 Sanborn, M.E., Wimpenny, J., Williams, C.D., Yamakawa, A., Amelin, Y., Irving, A.J.
676 and Yin, Q.-Z. (2019) Carbonaceous Achondrites Northwest Africa 6704/6693:
677 Milestones for Early Solar System Chronology and Genealogy. Geochimica et
678 Cosmochimica Acta 245, 577-596.
679 Schiller, M., Van Kooten, E., Holst, J.C., Olsen, M.B. and Bizzarro, M. (2014) Precise
680 measurement of chromium isotopes by MC-ICPMS. Journal of analytical atomic
681 spectrometry 29, 1406-1416.
682 Schoenberg, R., Merdian, A., Holmden, C., Kleinhanns, I.C., Haßler, K., Wille, M. and
683 Reitter, E. (2016) The stable Cr isotopic compositions of chondrites and silicate
684 planetary reservoirs. Geochimica et Cosmochimica Acta 183, 14-30.
685 Schoenberg, R., Zink, S., Staubwasser, M. and Von Blanckenburg, F. (2008) The stable
686 Cr isotope inventory of solid Earth reservoirs determined by double spike MC-ICP-MS.
687 Chemical Geology 249, 294-306.
688 Schultz, L., Weber, H.W. and Franke, L. (2005) Rumuruti chondrites: Noble gases,
689 exposure ages, pairing, and parent body history. Meteoritics & Planetary Science 40,
690 557-571.

691 Schulze, H., Bischoff, A., Palme, H., Spettel, B., Dreibus, G. and Otto, J. (1994)
692 Mineralogy and chemistry of Rumuruti: The first meteorite fall of the new R chondrite
693 group. Meteoritics 29, 275-286.
694 Shen, J., Liu, J., Qin, L., Wang, S.J., Li, S., Xia, J., Ke, S. and Yang, J. (2015)
695 Chromium isotope signature during continental crust subduction recorded in
696 metamorphic rocks. Geochemistry, Geophysics, Geosystems 16, 3840-3854.
697 Shen, J., Xia, J., Qin, L., Carlson, R.W., Huang, S., Helz, R.T. and Mock, T.D. (2019)
698 Stable chromium isotope fractionation during magmatic differentiation: Insights from
699 Hawaiian basalts and implications for planetary redox conditions. Geochimica et
700 Cosmochimica Acta.
701 Shima, M. and Honda, M. (1966) Distribution of spallation produced chromium
702 between alloys in iron meteorites. Earth and Planetary Science Letters 1, 65-74.
703 Shukolyukov, A. and Lugmair, G. (2006) Manganese–chromium isotope systematics of
704 carbonaceous chondrites. Earth and Planetary Science Letters 250, 200-213.
705 Sossi, P., Moynier, F. and van Zuilen, K. (2018) Volatile loss following cooling and
706 accretion of the Moon revealed by chromium isotopes. Proceedings of the National
707 Academy of Sciences 115, 10920-10925.
708 Sossi, P.A., Klemme, S., O'Neill, H.S.C., Berndt, J. and Moynier, F. (2019) Evaporation
709 of moderately volatile elements from silicate melts: experiments and theory.
710 Geochimica et Cosmochimica Acta 260, 204-231.
711 Trinquier, A., Birck, J.-L. and Allègre, C.J. (2006) The nature of the KT impactor. A 54
712 Cr reappraisal. Earth and Planetary Science Letters 241, 780-788.
713 Trinquier, A., Birck, J.-L. and Allègre, C.J. (2007) Widespread 54Cr heterogeneity in
714 the inner solar system. The Astrophysical Journal 655, 1179-1185.
715 Trinquier, A., Birck, J.L., Allègre, C.J., Göpel, C. and Ulfbeck, D. (2008) 53Mn–53Cr
716 systematics of the early Solar System revisited. Geochimica et Cosmochimica Acta 72,
717 5146-5163.
718 Trinquier, A., Elliott, T., Ulfbeck, D., Coath, C., Krot, A.N. and Bizzarro, M. (2009)
719 Origin of Nucleosynthetic Isotope Heterogeneity in the Solar Protoplanetary Disk.
720 Science 324, 374-376.
721 Wang, X., Planavsky, N.J., Reinhard, C.T., Zou, H., Ague, J.J., Wu, Y., Gill, B.C.,
722 Schwarzenbach, E.M. and Peucker-Ehrenbrink, B. (2016) Chromium isotope
723 fractionation during subduction-related metamorphism, black shale weathering, and
724 hydrothermal alteration. Chemical Geology 423, 19-33.
725 Warren, P.H. (2011) Stable-isotopic anomalies and the accretionary assemblage of the
726 Earth and Mars: A subordinate role for carbonaceous chondrites. Earth and Planetary
727 Science Letters 311, 93-100.
728 Weisberg, M.K., Prinz, M., Kojima, H., Yanai, K., Clayton, R.N. and Mayeda, T.K.
729 (1991) The Carlisle Lakes-type chondrites: A new grouplet with high Δ17O and
730 evidence for nebular oxidation. Geochimica et Cosmochimica Acta 55, 2657-2669.
731 Wiechert, U., Halliday, A., Lee, D.-C., Snyder, G., Taylor, L. and Rumble, D. (2001)
732 Oxygen isotopes and the Moon-forming giant impact. Science 294, 345-348.

733 Wu, G., Zhu, J.-M., Wang, X., Johnson, T.M. and Han, G. (2020) High-Sensitivity
734 Measurement of Cr Isotopes by Double Spike MC-ICP-MS at the 10 ng Level.
735 Analytical Chemistry 92, 1463-1469.
736 Yamakawa, A., Yamashita, K., Makishima, A. and Nakamura, E. (2010) Chromium
737 isotope systematics of achondrites: Chronology and isotopic heterogeneity of the inner
738 solar system bodies. The Astrophysical Journal 720, 150.
739 Yamashita, K., Maruyama, S., Yamakawa, A. and Nakamura, E. (2010) 53Mn-53Cr
740 chronometry of CB chondrite: Evidence for uniform distribution of 53Mn in the early
741 solar system. The Astrophysical Journal 723, 20.
742 Yin, Q., Jacobsen, B., Moynier, F. and Hutcheon, I.D. (2007) Toward consistent
743 chronology in the early solar system: high-resolution 53Mn-53Cr chronometry for
744 chondrules. The Astrophysical Journal Letters 662, L43.
745 Yin, Q., Yamashita, K., Yamakawa, A., Tanaka, R., Jacobsen, B., Ebel, D., Hutcheon, I.
746 and Nakamura, E. (2009) 53Mn-53Cr Systematics of Allende Chondrules and epsilon
747 54Cr--Cap Delta17O Correlation in Bulk Carbonaceous Chondrites, Lunar and
748 Planetary Science Conference, p. 2006.
749 Young, E.D., Kohl, I.E., Warren, P.H., Rubie, D.C., Jacobson, S.A. and Morbidelli, A.
750 (2016) Oxygen isotopic evidence for vigorous mixing during the Moon-forming giant
751 impact. Science 351, 493-496.
752 Zhang, A.-C., Kawasaki, N., Kuroda, M., Li, Y., Wang, H.-P., Bai, X.-N., Sakamoto, N.,
753 Yin, Q.-Z. and Yurimoto, H. (2020) Unique angrite-like fragments in a CH3 chondrite
754 reveal a new basaltic planetesimal. Geochimica et Cosmochimica Acta 275, 48-63.
755 Zhu, K., Liu, J., Moynier, F., Qin, L., Alexander, C.M.O.D. and He, Y. (2019a)
756 Chromium isotopic evidence for an early formation of chondrules from the Ornans CO
757 chondrite. The Astrophysical Journal 873, 82.
758 Zhu, K., Moynier, F., Barrat, J.-A., Wielandt, D., Larsen, K. and Bizzarro, M. (2019b)
759 Timing and origin of the angrite parent body inferred from Cr isotopes. The
760 Astrophysical Journal Letters 877, L13.
761 Zhu, K., Moynier, F., Schiller, M. and Bizzarro, M. (2020a) Dating and tracing the
762 origin of enstatite chondrite chondrules with Cr isotopes. The Astrophysical Journal
763 Letters 894, L26.
764 Zhu, K., Moynier, F., Schiller, M., Wielandt, D., Larsen, K., van Kooten, E. and
765 Bizzarro, M. (2020b) Chromium isotopic constraints on the origin the ureilite parent
766 body. The Astrophysical Journal 888, 126.
767 Zhu, K., Sossi, P.A., Siebert, J. and Moynier, F. (2019c) Tracking the volatile and
768 magmatic history of Vesta from chromium stable isotope variations in eucrite and
769 diogenite meteorites. Geochimica et Cosmochimica Acta 266, 598-610.

770